Biochimica et Biophysica Acta 1838 (2014) 3061–3068

Contents lists available at ScienceDirect

Biochimica et Biophysica Acta

journal homepage: www.elsevier.com/locate/bbamem

Structural dynamics of the cell wall precursor lipid II in the presence and absence of the lantibiotic nisin

Dennis C. Koch [a], Thomas H. Schmidt [a], Hans-Georg Sahl [b], Ulrich Kubitscheck [c], Christian Kandt [a,*]

[a] Computational Structural Biology, Department of Life Science Informatics B-IT, Life & Medical Sciences (LIMES) Institute, Rheinische Friedrich Wilhelms-University Bonn, Dahlmannstraße 2, 53113 Bonn, Germany
[b] Institute for Medical Microbiology, Immunology and Parasitology, Pharmaceutical Microbiology Unit, Meckenheimer Allee 168, Rheinische Friedrich-Wilhelms-University Bonn, 53115 Bonn, Germany
[c] Biophysical Chemistry, Department of Physical and Theoretical Chemistry, Rheinische Friedrich Wilhelms-University Bonn, Wegelerstraße 12, 53115 Bonn, Germany

ARTICLE INFO

Article history:
Received 24 June 2014
Received in revised form 23 July 2014
Accepted 25 July 2014
Available online 12 August 2014

Keywords:
Molecular dynamics simulation
Lipid II
Nisin
Lipid membrane
Molecular modeling
Antimicrobial peptides

ABSTRACT

Representing a physiological "Achilles' heel", the cell wall precursor lipid II (L_{II}) is a prime target for various classes of antibiotics. Over the years L_{II}-binding agents have been recognized as promising candidates and templates in the search for new antibacterial compounds to complement or replace existing drugs. To elucidate the molecular structural basis underlying L_{II} functional mechanism and to better understand if and how lantibiotic binding alters the molecular behavior of L_{II}, we performed molecular dynamics (MD) simulations of phospholipid membrane-embedded L_{II} in the absence and presence of the L_{II}-binding lantibiotic nisin. In a series of 2×4 independent, unbiased 100 ns MD simulations we sampled the conformational dynamics of nine L_{II} as well as nine L_{II}–nisin complexes embedded in an aqueous 150 mM NaCl/POPC phospholipid membrane environment. We found that nisin binding to L_{II} induces a reduction of L_{II} mobility and flexibility, an outward shift of the L_{II} pentapeptide, an inward movement of the L_{II} disaccharide section, and an overall deeper insertion of the L_{II} tail group into the membrane. The latter effect might indicate an initial step in adopting a stabilizing, scaffold-like structure in the process of nisin-induced membrane leakage. At the same time nisin conformation and L_{II} interaction remain similar to the 1WCO L_{II}–nisin NMR solution structure.

1. Introduction

The discovery, development and clinical exploitation of antibiotics count among the most significant medical advances of the previous century. Reducing the mortality rate from bacterial infections and diseases, antibiotics have become cornerstones of modern medicine required by many common procedures such as transplantation, chemotherapy for cancer or surgery [1]. However, antibiotics lose their efficiency after a period of months to years [2–4], eventually producing new strains of bacteria resistant to the given drug. Since old antibiotics lose their efficiency faster than new ones can be developed [5], there is currently no antibiotic in clinical use, to which resistance has not yet been reported [6,7]. Even in developed countries bacterial infections again count among the top five causes of death, while at the same time the approval rates of new antibiotics have been declining continuously since the 1980s [8,9]. As the need to discover and develop new agents is paramount for modern biomedical research, a detailed understanding of the molecular basis of antibiotics resistance is essential. Discovering and developing new antibiotics can be done designing a drug specifically aiming at a previously identified potential target, e.g. an antibacterial defense mechanism such as multidrug efflux transporters of the resistance nodulation division protein super family [10,11]. Alternatively, an existing antimicrobial compound, that is for example part of an antibacterial attack mechanism, can be optimized to increase its efficiency and band width. For both strategies, however, a detailed understanding of the molecular interactions between drug and target is required.

In bacteria, lipid II (L_{II}) is a central component of the enzymatic cell wall building machinery, translocating the monomeric peptidoglycan units from the cytoplasm to the outside of the membrane. L_{II} consists of a long undecaprenyl (bactoprenol) hydrocarbon chain that is coupled to a monomeric peptidoglycan unit through a pyrophosphate linker. The peptidoglycan unit is the basic building block of the bacterial cell wall and comprises the two amino sugars N-acetylglucosamine (GlcNAc) and N-acetylmuramic acid (MurNAc), with a pentapeptide bound to the latter (Fig. 1a). Due to its function, L_{II} represents a primary molecular target for a large number of antibiotics [12].

Nisin is a lantibiotic produced by numerous strains of lactic acid bacteria. Lantibiotics are antimicrobial peptides comprising intramolecular rings formed by the thioether amino acids lanthionine and

* Corresponding author.
E-mail address: chkandt@mail.de (C. Kandt).

http://dx.doi.org/10.1016/j.bbamem.2014.07.024
0005-2736/

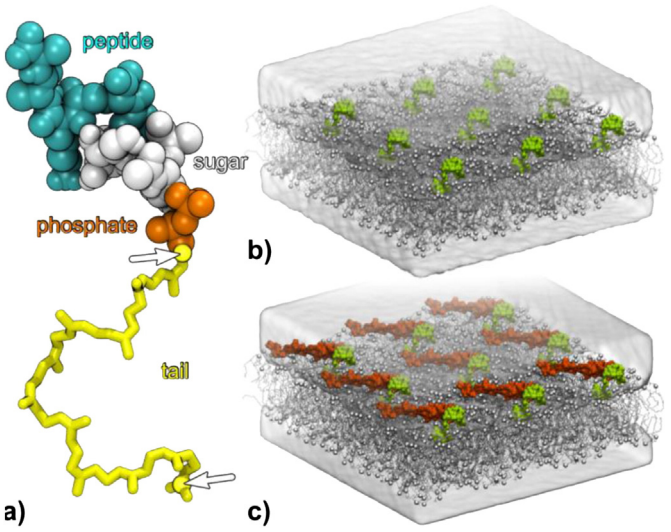

Fig. 1. Lipid II domain structure (a) and simulation starting structures (b, c). To better understand the structural basis underlying the functional mechanism of the cell wall precursor lipid II we computed samples of its dynamics in an aqueous 150 mM NaCl/POPC phospholipid membrane environment in the absence (b) and (c) presence of the lantibiotic nisin. For each system we performed a series of 4 independent, unbiased 100 ns molecular dynamics simulations. The arrows in (a) mark the lipid II atoms used for the tail length vs. membrane insertion depth analysis shown in Fig. 6.

3-methyllanthionine [13,14]. Belonging to the class of type-A lantibiotics, elongated, screw-shaped peptides with a positive net charge, nisin is active against a wide range of Gram-positive bacteria [15,16]. Highly polar, antimicrobial peptides like nisin often form amphipathic structures when interacting with membranes [17,18], and nisin kills bacteria by perforating the cell membrane [19,20], targeting L_{II}. The pyrophosphate of L_{II} was identified as the binding site for nisin, around which two of nisin's lanthionine rings form a cage-like structure [21]. Numerous studies showed that nisin binding to L_{II} results in membrane pore formation [14,22–24], a process in which L_{II} not only acts as mere receptor but is an active constituent of the L_{II}–nisin pore whose stability depends on the length of the L_{II} alkyl chain [25]. Beyond altering the membrane the specific interaction of nisin and L_{II} leads to the inhibition of cell wall biosynthesis, because L_{II} is sequestered and removed from the enzymatic reaction cycle [22]. Notably, when the interaction of nisin with bacterial or artificial membranes was directly observed using fluorescently labeled nisin, the peptides were not homogeneously distributed on the membrane, but rather clustered in large aggregates [23,26]. While this might be explicable in bacterial membranes, it is astonishing that this was also observed for L_{II}-containing model membranes.

To obtain insight into the molecular mechanism, by which nisin – just binding to the pyrophosphate unit of L_{II} – can produce the discussed very diverse effects, we performed MD simulations to understand if and how nisin alters the molecular behavior of membrane-embedded L_{II}. Whereas previous computational studies have focused either on single L_{II} molecules in different bilayer environments [27] or on L_{II} interacting with vancomycin [28,29], here we sampled L_{II} conformational dynamics in two series of four unbiased, independent 100 ns MD simulations of nine L_{II} as well as nine L_{II}–nisin complexes embedded in a POPC membrane in physiological salt solution. We find that nisin alters L_{II} membrane insertion inducing (i) longer prenyl tail conformations intruding deeper into the membrane; (ii) an outwards shift of the L_{II} pentapeptide section while (iii) the disaccharide section inserts deeper into the membrane. In addition, complexation with nisin lowers the L_{II} diffusion speed as well as the overall volume occupied by L_{II}. At the same time the nisin conformation and key residues of L_{II} interaction remained similar to the known 1WCO L_{II}–nisin NMR solution structure [21].

2. Materials and methods

2.1. Simulation details

MD simulations were performed employing *GROMACS* version 4.0.3 [30,31] and the GROMOS96 force field with the 54a7 parameter set [32]. In all simulations standard protonation states were assumed for titratable residues and all bond lengths were constrained by LINCS [33] so that an integration time step of 2 fs could be chosen. Systems were simulated at 300 K, maintained separately for protein, lipids and water + ions by a Berendsen thermostat [34] with a time constant (τ_T) of 0.1 ps. Pressure coupling was done employing a Berendsen barostat [34] using a 1 bar reference pressure and a time constant of 4 ps. To permit bilayer fluctuations in the membrane plane semiisotropic pressure coupling was used. Electrostatic interactions were calculated using particle mesh Ewald (PME) Summation [35,36], and twin range cutoffs of 1.0 and 1.4 nm were applied for computing the van der Waals interactions.

Starting point for all simulations was conformer 1 of the 1WCO L_{II}–nisin NMR solution structure [21] after completing the truncated 3LII variant using the full length L_{II} structural model (Fig. 1a) by Jia and co-workers [28], from which we also adapted the simulation parameters. Details on the nisin simulation parameters can be found in the supplemental material and supplemental Fig. 1. Simulation systems were constructed inserting a single L_{II}–nisin or L_{II}, respectively, into a pre-equilibrated 128 lipid POPC bilayer patch [37] using *InflateGRO2* [38]. In this process 2 POPC lipids were deleted from the L_{II}-containing leaflet. Next, each simulation system was extended three times in X and Y direction using GROMACS tool *genconf* and subsequently solvated in an aqueous 150 mM NaCl solution yielding a total charge of 0. The final simulation systems comprise 9 L_{II}; 1134 POPC; 5,9150 H_2O; 335 Na^+ and 308 Cl^- at a total system size of 238,357 atoms (Fig. 1b) as well as 9 L_{II}–nisin; 1134 POPC; 57,787 H_2O; 308 Na^+ and 310 Cl^- at a total system size of 236,799 atoms (Fig. 1c). Following steepest descent energy minimization and 0.5 ns equilibration at constant volume and temperature, four independent, unbiased 100 ns MD runs were initiated for each simulation system using different random seed numbers in generating the starting velocities.

2.2. Analysis

Using the GROMACS tool *g_density* [30,31] we computed 1-dimensional density profiles to determine the overall distribution of the system components. After least-square fitting on the POPC phosphorous atoms partial densities were computed for the POPC bilayer, L_{II}, its structural domains and nisin using the last 50 ns of the trajectories. To gain further insight into L_{II}-interaction with the membrane and nisin, we computed the average amount of ≤4 Å heavy atom contacts between L_{II}'s four structural domains (peptide section, dissacharide, phosphate and hydrophobic tail) and the POPC head and tail groups as well as nisin. The analysis was performed on the last 50 ns of the trajectories using the GROMACS tool *g_mindist* [30,31] as well as *xmgrace* for averaging and visualization.

In order to elucidate whether nisin alters the conformational dynamics of L_{II}'s hydrophobic tail, we computed for all trajectories the distance between the first and last atom of the L_{II}-tail (Fig. 1a) as well as monitored the Z coordinate of the LII-tail tip atom. Computed over the last 50 ns, the analysis was performed for all trajectories calculating and plotting the resulting tail length vs. insertion depth distributions in *QtiPLOT*.

Assessing the amount of space occupied by L_{II}, its structural domains and nisin, each trajectory was converted to a voxel-based representation of spatial density, for which profiles of cross-sectional area along the membrane normal were computed. Following the initial least square alignment of the POPC phosphorus atoms, the last 50 ns of each of the 36 L_{II} and L_{II}–nisin molecules were aligned using lateral translations